Exceptional melt pond occurrence in the years 2007 and 2011 on the Arctic sea ice revealed from MODIS satellite data

Anja Rösel[1] and Lars Kaleschke[1]

Received 30 December 2011; revised 23 February 2012; accepted 18 March 2012; published 12 May 2012.

[1] Melt ponds contribute to the ice-albedo feedback as they reduce the surface albedo of sea ice, and hence accelerate the decay of Arctic sea ice. Here, we analyze the melt pond fraction, retrieved from the MODIS sensor for the years 2000–2011 to characterize the spatial and temporal evolution. A significant anomaly of the relative melt pond fraction at the beginning of the melt season in June 2007 is documented. This is followed by above-average values throughout the entire summer. In contrast, the increase of the relative melt pond fraction at the beginning of June 2011 is within average values, but from mid-June, relative melt pond fraction exhibits values up to two standard deviations above the mean values of 30 ± 1.2% which are even higher than in Summer 2007.

Citation: Rösel, A., and L. Kaleschke (2012), Exceptional melt pond occurrence in the years 2007 and 2011 on the Arctic sea ice revealed from MODIS satellite data, *J. Geophys. Res.*, *117*, C05018, doi:10.1029/2011JC007869.

1. Introduction

[2] In the Arctic summer, melt ponds commonly occur on Arctic sea ice and cover up to 50–60% of the sea ice area [*Fetterer and Untersteiner*, 1998; *Eicken et al.*, 2004]. Melt ponds are defined as an accumulation of meltwater on sea ice, mainly due to melting snow, but in the more advanced stages also due to the melting of sea ice. The distribution on the ice, the size and the depth of the ponds, as well as the color is very variable and depending on topography, surface and atmospheric conditions. On the flat topography of first-year ice it is possible that the melt pond fraction rises up to 90% [*Perovich et al.*, 2011b].

[3] Literature values of spectral and total albedo for various Arctic surface types, acquired on field campaigns and measurements, range from 0.06 for open water over 0.29 for mature melt ponds to 0.87 for new snow [e.g., *Grenfell and Maykut*, 1977; *Grenfell and Perovich*, 1984; *Warren*, 1982; *Perovich*, 1996; *Perovich et al.*, 2002b; *Brandt et al.*, 2005].

[4] To study the spectral behavior of melt ponds and their influence on the declining surface albedo during summer, several field experiments and ship observations took place on various locations of the Arctic [e.g., *Perovich et al.*, 2002a, 2002b; *Sankelo et al.*, 2010; *Nicolaus et al.*, 2010; *Itoh et al.*, 2011].

[5] The existence of melt ponds on Arctic sea ice causes a decrease of the surface albedo from a range of 0.8–0.9 to a range of 0.3–0.6 due to a higher absorption of the incoming radiation. This effect initiates additional heat uptake [*Curry et al.*, 1995; *Perovich and Tucker*, 1997]. Therefore, melt ponds have a significant influence on the amount of sea ice melt [*Perovich et al.*, 2002a; *Tschudi et al.*, 2008], on Earth's radiation balance [*Maslanik et al.*, 2007; *Perovich et al.*, 2007; *Nicolaus et al.*, 2010], and the potential loss of a multiyear ice coverage [*Maslanik et al.*, 2007; *Perovich et al.*, 2007; *Nicolaus et al.*, 2010; *Kwok and Untersteiner*, 2011; *Serreze and Barry*, 2011]. Melt ponds absorb more solar radiation than unponded sea ice, promoting further localized melting [*Ehn et al.*, 2011]. Furthermore, the transmission of incident irradiance through ponded ice is up to an order of magnitude greater than through bare ice [*Frey et al.*, 2011; *Ehn et al.*, 2011].

[6] A quantification of the overall distribution of melt ponds would be helpful to constrain the role of sea ice for the Arctic amplification and Earth's climate system [e.g., *Holland et al.*, 2006; *Eisenman and Wettlaufer*, 2009; *Notz*, 2009; *Serreze*, 2011; *Serreze et al.*, 2011; *Kurtz et al.*, 2011; *Perovich et al.*, 2011a]. Until now, statements about the melt pond distribution in the Arctic can only be made from the attempts to model melt ponds [*Lüthje et al.*, 2006; *Pederson et al.*, 2009; *Scott and Feltham*, 2010; *Skyllingstad et al.*, 2009; *Flocco et al.*, 2010]. A realistic presentation of melt pond fractions in the Arctic is only be possible with observations on a large scale over at least one melting period. Therefore, it is important to use remote sensing techniques that are applicable to detect the evolution of melt ponds. To survey melt ponds Arctic-wide, approaches regarding the use of satellite data have been developed by *Markus et al.* [2003]; *Tschudi et al.* [2008]; *Rösel and Kaleschke* [2011] and *Rösel et al.* [2012].

[7] A scientific debate is ongoing with respect to the role of clear skies anomalies. For example, *Schweiger et al.* [2008] and *Lindsay et al.* [2009] demonstrated with experiments from a dynamic ice-ocean model that the negative cloud anomaly over the Arctic in 2007 did not contribute substantially to the record sea ice extent minimum of the same year. In contrast, analysis from observations and reanalysis data reveal in a significant impact of negative cloud cover anomalies on the surface energy budget [e.g., *Kay et al.*, 2008; *Walsh et al.*, 2009; *Perovich et al.*, 2008; *Howell et al.*, 2010].

[1]Institute of Oceanography, University of Hamburg, Hamburg, Germany.

Corresponding author: A. Rösel, Institute of Oceanography, University of Hamburg, Bundesstr. 53, D-20146 Hamburg, Germany. (anja.roesel@zmaw.de)

0148-0227/12/2011JC007869

Table 1. Spectral Reflectances, r_i, of Surface Types Used in the Unmixing Algorithm[a]

MODIS Band	Bandwidth (nm)	Resolution (m)	Pond r_i	Snow/Ice r_i	Open Water r_i
3	459–479	500	0.22	0.95	0.08
1	620–670	250	0.16	0.95	0.08
2	841–876	250	0.07	0.87	0.08

[a]Reprinted from *Tschudi et al.* [2008] with permission from Elsevier.

[8] The extreme sea ice loss in the last decade is induced by multiple factors. One factor is a thinner ice cover [*Kwok and Untersteiner*, 2011] that is more susceptible to the enhanced summer melt [*Levermann et al.*, 2011]. The loss of multiyear sea ice and the associated increase of first-year ice [*Maslanik et al.*, 2011] enhances melt pond formation [*Agarwal et al.*, 2011; *Ehn et al.*, 2011].

[9] We hypothesize that the timing of melt pond formation determines the cumulative short wave radiation uptake. Therefore the occurrence of melt ponds is a major factor influencing the September extent.

[10] For this study we use the melt pond fraction of the entire Arctic retrieved from MODIS (Moderate Resolution Image Spectrometer) satellite data for the time range from 2000 to 2011 [*Rösel et al.*, 2012]. During this time, two extreme minimum annual sea ice extents were recorded in the years 2007 and 2011. In this study, we analyze the seasonal evolution of melt ponds, focusing on the melt pond fraction during the extreme events in the years 2007 and 2011.

2. Methods and Data

[11] Melt pond fractions have been derived from the multispectral optical MODIS sensor by making use of the different spectral behavior of melt ponds comparing to other sea ice surface features like open water or snow and ice [*Tschudi et al.*, 2008; *Rösel et al.*, 2012]. The MODIS-based melt pond data set we used for this study is built on a three-class-surface model, assuming melt ponds, open water, and snow and ice as surface types of the Arctic Ocean. The method to retrieve these surface fractions for an 8-day interval with 12.5 km resolution is described in detail in *Rösel et al.* [2012] and will be shortly summarized:

[12] The melt pond fraction was derived by using a spectral unmixing algorithm, motivated by the approach of *Tschudi et al.* [2008]. This algorithm consists of a system of linear equations which describes the fractions of three surface types on the sea ice, namely open water (W), melt pond (M), and snow and ice (I)

$$\begin{aligned} A_W r_W(\lambda_1) + A_M r_M(\lambda_1) + A_I r_I(\lambda_1) &= R(\lambda_1), \\ A_W r_W(\lambda_3) + A_M r_M(\lambda_3) + A_I r_I(\lambda_3) &= R(\lambda_3), \\ A_W r_W(\lambda_4) + A_M r_M(\lambda_4) + A_I r_I(\lambda_4) &= R(\lambda_4), \\ A_W + A_M + A_I &= 1, \end{aligned} \tag{1}$$

where $R(\lambda_k)$ is the reflectance of each band k = 1, 3, and 4, with the corresponding wavelengths $r(\lambda_1)$ = 459–479 nm, $r(\lambda_3)$ = 620–670 nm and $r(\lambda_4)$ = 841–876 nm, for each MODIS pixel. A is the fractional coverage of each surface type for each band, and $r(\lambda_k)$ represents the spectral reflectance for each surface type. The specific reflectance values for the three surface types used for these equations are gained from field observations listed in Table 1.

[13] The set of linear equation (1) is overdetermined, thus we consider it as an optimization problem that needs to be solved in a least-square sense. Additionally, equation (1) show linear dependence, especially for the surface types open water and melt ponds. To comply with the physical principles, it is necessary to constrain the interval of the solution between zero and one for each class. A Lagrangian operator in form of a sigmoid function is implemented as a side condition in a cost function [*Rösel et al.*, 2012]. To evade the high computational costs that were caused by this solution and to speed up processing, an artificial neural network (ANN) was trained successfully [*Rösel et al.*, 2012]. With this approach we obtained a multiannual melt pond data set of the entire Arctic from MODIS data. We validated the relative melt pond fractions with three different data types from local observations: First, we used aerial photos from the MELTEX campaign in the Beaufort Sea in June 2008. The RMSE of the comparison of two MELTEX data sets with two MODIS melt pond sets were 11.2% and 10.6%, respectively. Secondly, we compared analyzed intelligence satellite data with a resolution of 1 m × 1 m of three sites in the Arctic Ocean for the years 2000 and 2001. The RMSE for the data of all sites and both years amounts to 10.7%.Thirdly, ship observation data from the HOTRAX 2005 cruise in the Arctic Ocean were used for validation. The determined RMSE between ship and satellite data resulted in 3.8%.

[14] To obtain the relative melt pond fraction $\widetilde{A_M}$, we scale the melt pond data set with the sea ice concentration, created by using the MODIS open water fraction

$$\widetilde{A_M} = A_M(1 - A_W). \tag{2}$$

Hence, only melt pond fractions located on sea ice are considered. Additionally, we calculate the amount of pixel used for creating the mean value of the relative melt pond fraction in the 12.5-km gridding routine. This product can be used for further analysis to mask the melt pond fraction fraction on a 12.5 km grid and it can also be considered as an indicator how trustworthy the result of the coarse grid is. A large amount of valid observations indicates high data quality; whereas, a low amount of valid observations indicates low data quality. To avoid low data quality, we select only grid cells, that contain more than 50% cloud free pixel [*Rösel et al.*, 2012]. To gain absolute values of the total melt pond area A_{Mtotal} (in further context called absolute melt pond area), the relative melt pond fraction $\widetilde{A_M}$ is scaled with the according sea ice area $A_{\mathrm{SeaIceArea}}$

$$A_{\mathrm{Mtotal}} = \widetilde{A_M} A_{\mathrm{SeaIceArea}}. \tag{3}$$

Note, that in this case we use the sea ice area from NSIDC [*Fetterer et al.*, 2002] and not from the MODIS sea ice concentration data, because the MODIS data contain data gaps due to clouds and unavailable data.

3. Results

[15] Figure 1 shows the spatial and temporal evolution of the melt pond fraction in the Arctic, between May 9 and September 6 for the year 2011. In the first week of the seasonal cycle, starting on May 9, melting features appear only at the ice edges in the Greenland Sea, Kara Sea, and Barents

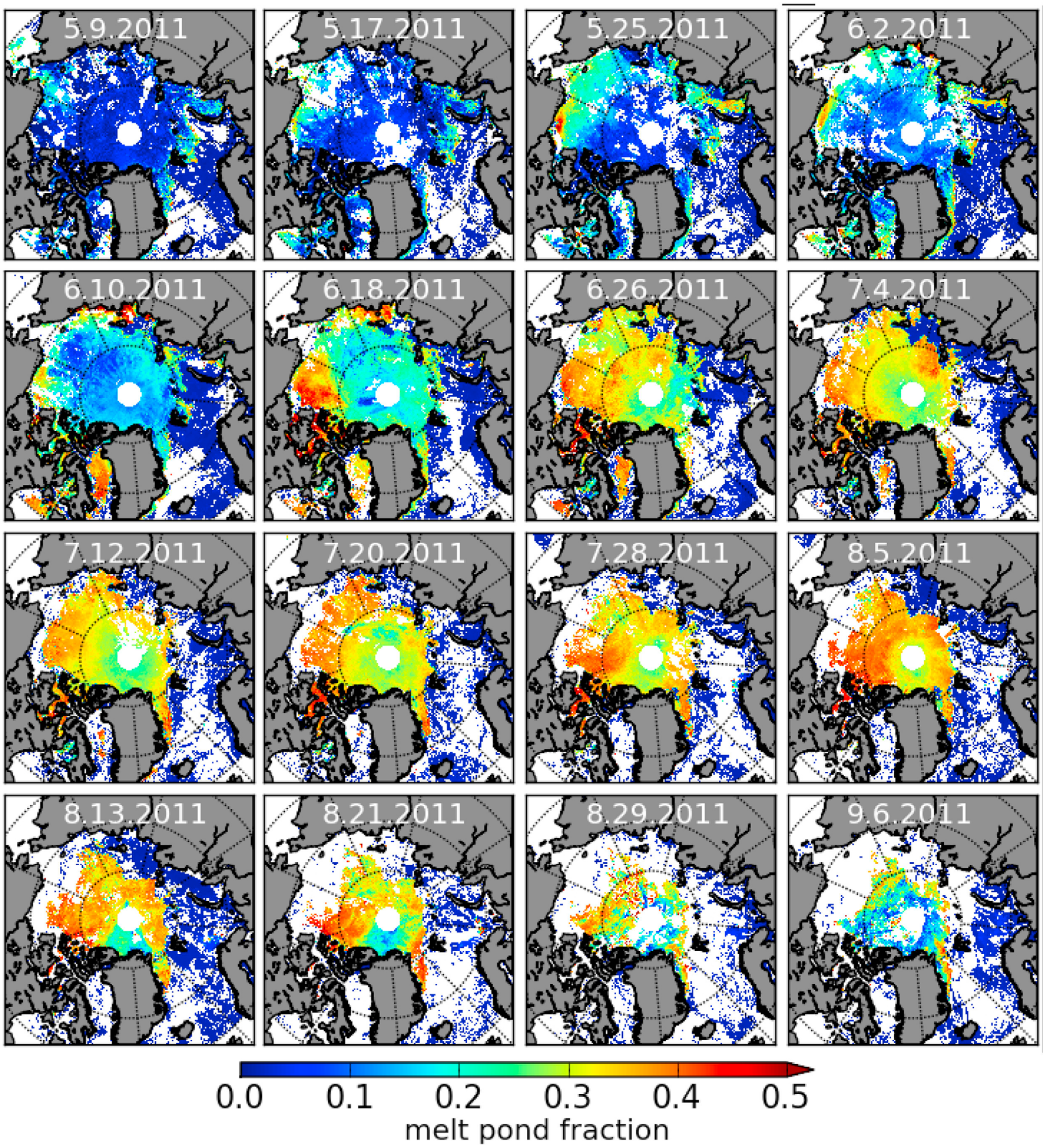

Figure 1. Seasonal cycle of the melt pond fraction on sea ice from MODIS satellite data for the Arctic in 2011. Dates given at the top of the images denote the start date of the used 8-day period. White areas display data gaps.

Sea, Bering Strait and Davis Strait and in Hudson Bay. Melt pond fraction continuously increases and on June 18 the melt pond fraction rises intensely in the Canadian Archipelago and the Beaufort Sea (see also Figure 2).

[16] Highest melt pond fractions in the Canadian Archipelago occur in both years, 2007 and 2011, in the week after June 18 (Figure 2). In contrast, melt pond fractions with values above 30% emerge in different regions when comparing the two years:

[17] In 2007, an expansion of melt ponds mainly occurs in first-year ice areas—namely in the Beaufort Sea, Chukchi Sea, and Laptev Sea, whereas in 2011, an intensive melt pond formation is concentrated only in southern parts of Beaufort Sea and Laptev Sea, as well as Baffin and Hudson Bay. Areas with melt pond fractions less than 20% in 2007 can only be found in multiyear ice regions north of the Canadian Archipelago and Greenland. In contrast, melt pond fractions with values below 20% are spreading from the northern Beaufort Sea over the Chukchi Sea to the Laptev Sea, and can also be observed in the Central Arctic.

[18] The areal extent of melt pond fraction increases in the subsequent weeks (Figure 1) and melt ponds progress into higher latitudes. However, in the same time period, total sea ice area is declining—therefore we consider both, relative melt pond fraction and absolute melt pond area (Figures 3a and 3b).

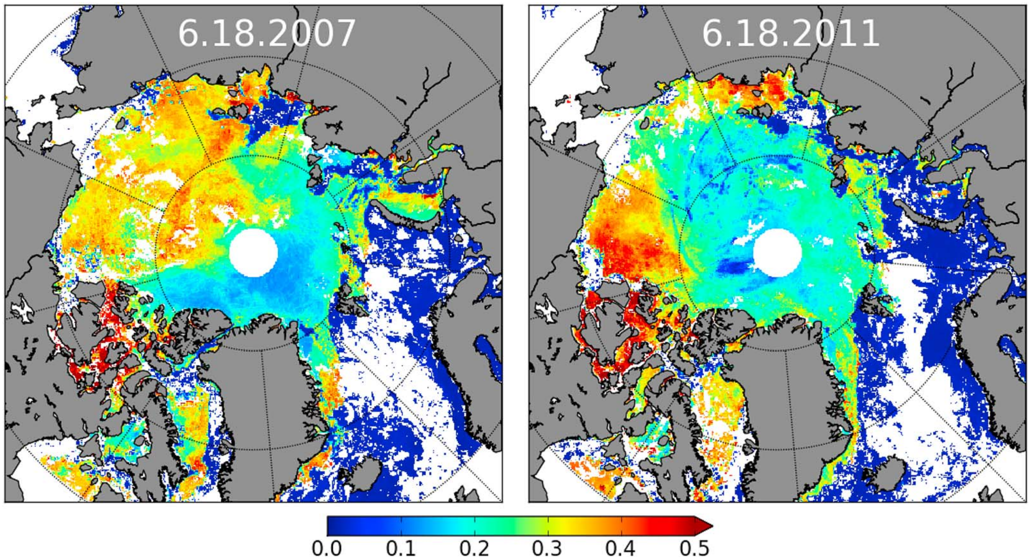

Figure 2. Comparison of the spatial melt pond fraction from the data sets of (left) June 18 2007 and (right) June 18 2011.

[19] Figure 3a illustrates multiannual mean relative melt pond fractions of the Arctic Ocean and the individual annual cycles for 2000 to 2011. The relative mean melt pond fraction shows a strong increase in June with a maximum of 30% lasting from the end of June until the beginning of August. Seasonal cycles of the years 2007 and 2011 both begin below the average curve of relative melt pond fraction. With the beginning of June, relative melt pond fraction in 2007 has its highest increase and rises above average values. A first maximum of relative melt pond fraction in 2007 is reached in mid-June, which is followed by above-average values in July and August. In contrast to 2007, relative melt pond fraction in 2011 shows a smoother increase at the beginning of the melt season and exceeds the mean values in mid-June. From this point in time the curve of 2011 remains up to two standard deviations above average (30 ± 1.2%) and even above the high values of 2007.

[20] Figure 3b depicts absolute melt pond areas for all years of the Arctic region. There is evidence that annual sea ice extent has a strong influence on total melt pond area. Both years, 2007 and 2011 begin below the average curve of total melt pond area due to negative sea ice extent anomalies. Additionally, strong increases of melt ponds in June and their early occurrence (Figure 3a) have a severe influence on total melt pond area (Figure 3b). The observed maximum melt pond area in 2011 is 2.5 million km^2 and amounts 0.4 million km^2 more than the average maximum of all years. The 2007 maximum, with 2.4 million km^2, lies slightly lower than 2011 between the maximum of 2011 and the average value of 2.1 million km^2. Note that until the 2007 maximum

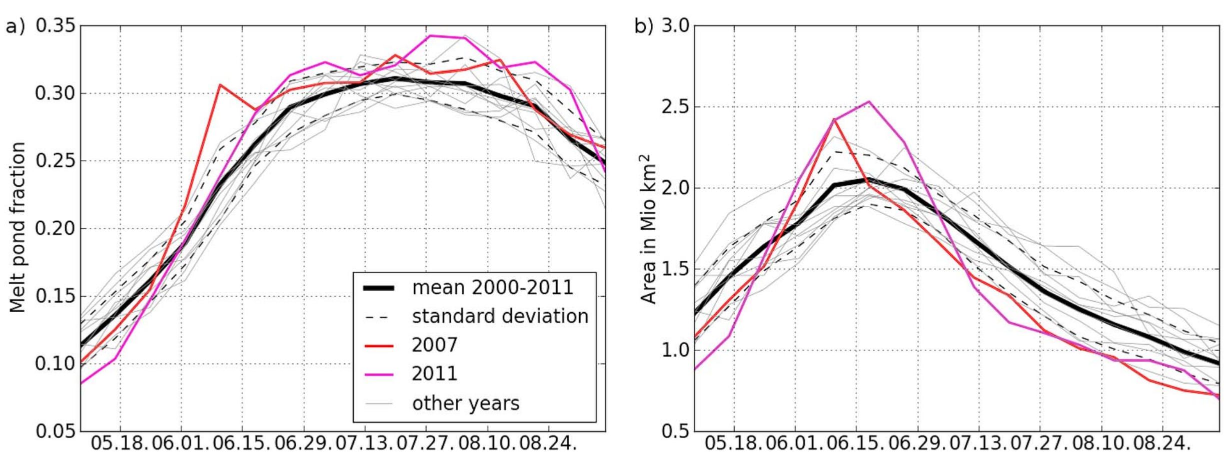

Figure 3. (a) Multiyear mean relative melt pond fraction (black line) with standard deviation (dashed line) and (b) mean sea ice area covered with melt ponds (black line) with standard deviation (dashed line) for the time period 2000–2011 relative to the sea ice area for the entire Arctic. The light gray lines display the development of melt ponds for the single years. The years 2007 (red) and 2011 (magenta) are highlighted for comparison.

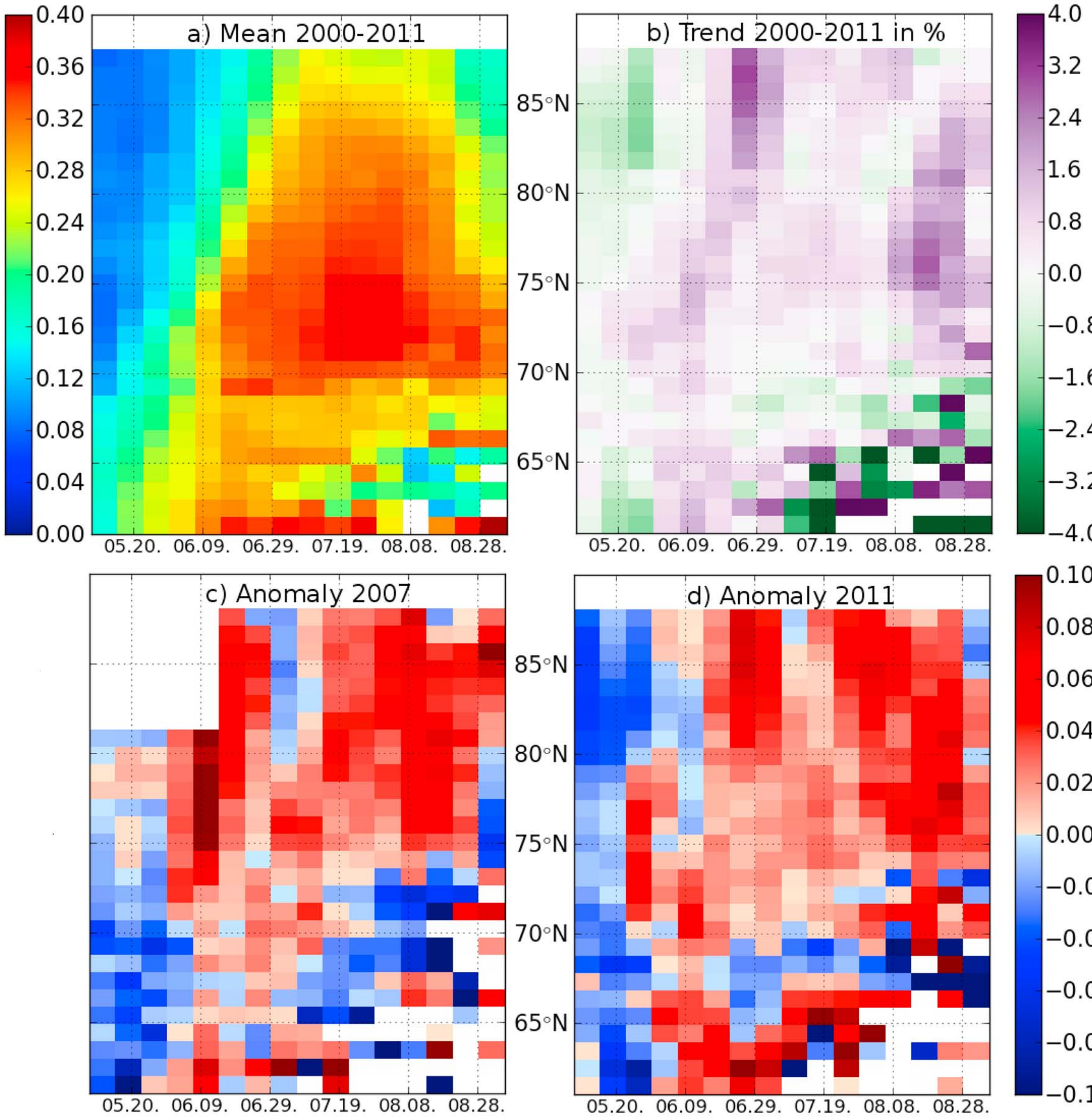

Figure 4. (a) Zonal mean of relative melt pond fraction over the entire Arctic from 2000–2011, (b) trends of zonal relative melt pond fraction over the period from 2000–2011, (c) anomaly of relative melt pond fraction in 2007 and (d) anomaly of relative melt pond fraction in 2011.

value in the first week of June, both graphs for 2007 and 2011 exhibit values in the same range. After the first week of June total melt pond area for 2007 reaches its maximum, whereas it increases until mid-June in 2011. Due to the outstanding decrease of sea ice area in 2007 and 2011, total melt pond areas drop at end of June below the average value in both years.

[21] Figure 4a displays the zonal mean of melt ponds for the last 12 years. This Hovmoeller diagram demonstrates a dependence of the temporal development of melt ponds from the geographical latitude. The maximum of the averaged relative melt pond fraction is located from mid-June to mid-August in the latitudes between 70° and 80°N. A second maximum in the lower latitudes (60°–62°N) in June indicates the coastal melting and the melt ponds in Hudson and Baffin Bay. Patterns in 2007 and 2011 look very similar (see Figures 4c and 4d), although both exhibit higher relative melt pond fractions in high latitudes than the mean reference period 4a), and in 2011 melting in low latitudes is more pronounced. As in Figure 3a, largest differences in 2007 to the mean values occur at the beginning of the melt season between 70° and 80°N. 2007 and 2011 show higher relative melt pond fractions between 80° and 90°N, especially in mid-June (see Figures 4c and 4d). Positive significant trends of up to 3% at a 95% significance-level can be identified in June and August in Figure 4b. For the trend calculations we define the melt pond fraction values of the year 2000 as 100% and calculate the deviation from this value for the following eleven years. These positive trends reflect the increase in the relative melt pond fraction at the beginning and the end of the

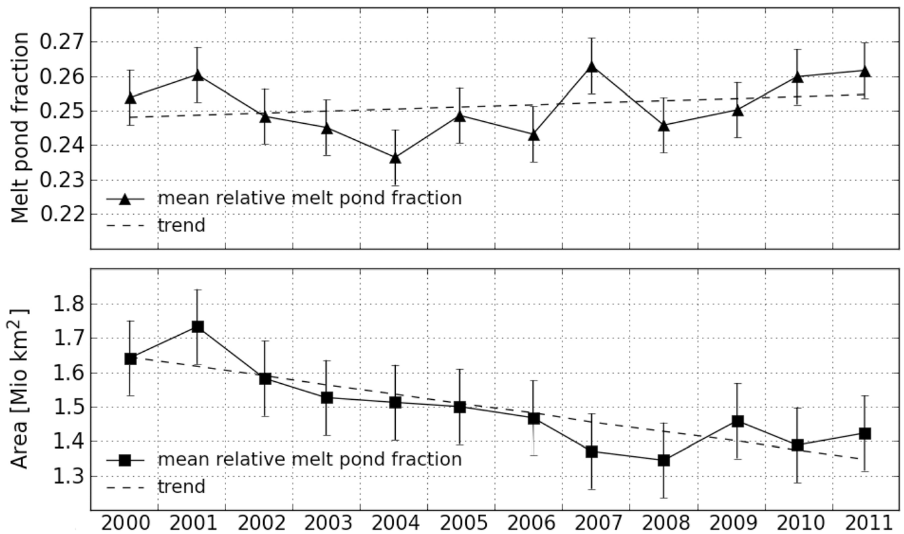

Figure 5. (top) Mean relative melt pond fraction and (bottom) mean absolute melt pond area for the years 2000–2011 for the entire Arctic with its standard deviations and trends.

melting period and indicates an earlier melt onset and a prolonged melting. The negative trends of −4% in August below 70°N depict the declining sea ice extent.

[22] Figure 5 displays a negative trend of the total melt pond area for entire time range. The mean relative melt pond fraction of all years is 25.1 ± 0.06%, the mean total melt pond area is 1.49 ± 0.11 million km^2. Although the time series with only twelve values is very short, the calculated trend of −16.4% for the decreasing mean melt pond area is statistically significant at the 90% significance-level, proved with the Cox and Stuart test. The mean melt pond area for 2011 (1.42 million km^2) is very close to the mean value, although in this year the overall maximum of the melt pond area was recorded in mid-June; but the low sea ice extent in late summer compensates the extreme values in early summer. The relative melt pond fraction exhibits a non-significant, slight upward trend of 2.4%, where the years 2007, 2010 and 2011 record the three highest values of the time series.

4. Discussion

[23] The weekly MODIS melt pond fractions used for this analysis is a composition of selected pixels from daily acquisitions. Validation studies of this product are described in a previous publication [*Rösel et al.*, 2012]. The comparison of MODIS melt pond fractions with (i) aerial photos from the MELTEX campaign in 2008 [*Birnbaum et al.*, 2009], (ii) sea ice observations from the HOTRAX 05 cruise [*Perovich et al.*, 2009] and (iii) sea ice melt pond statistics of different Arctic ocean sites during the summers of 2000 and 2001 from the National Snow and Ice Data Center (NSIDC) [*Fetterer et al.*, 2008] indicates a high accordance with a RMSE ranging from 3.8% to 11.2%.

[24] The observed differences between validation and MODIS data may result from the different spatial resolutions, from geolocation errors and/or time differences between observations and satellite acquisitions. Potential sources of errors are to be assumed in the atmospheric correction routines and influences of the viewing angles and the solar geometry. The BRDF correction of the MOD09 product is not performed on all areas of the Arctic sea ice, especially not over the deep ocean, because of the moving sea ice surface. For most of the areas, model results for first-year and multiyear ice are used as "a priori" estimates of the BRDF.

[25] Our assumption of a three-surface-class model also causes uncertainties regarding the different fractions, since the Arctic sea ice cover is actually a mosaic of various surface types—and not only melt ponds, snow and ice, and open water. The method described here is based on optical satellite data—therefore, melt pond fractions can only be identified from cloud free data. The used cloud mask, integrated into the MOD09 product, does not capture all actual present clouds, e.g. low-lying clouds were not filtered out and appear as highly reflecting surface features. Especially over highly reflecting surfaces like sea ice, the used cloud mask may have problems. To enhance data quality for this study, we applied a data mask with a 50% threshold of involved pixel after the gridding routine. In the 500 m grid, single pixels with a high melt pond signal occur often within cloudy fields or at the edges of the cloud mask. We assume, that these pixels are a misclassified cloud signal [*Rösel et al.*, 2012]. However, the existing problem of cloudy pixel in the initial data set can impact the melt pond fraction and should be considered.

[26] The initial MODIS product contains data gaps in terms of missing tiles. These gaps occur mainly in areas above 80°N in the years 2000, 2001, 2002 and 2007. We analyzed the influence of missing data for the time series analysis and found a negligible (below 1%) effect on the overall results. Also, cloud masking leads to a lack of data in the melt pond fraction. Smaller areas of missing data were interpolated by the gridding routine [*Rösel et al.*, 2012], areas larger than the 12.5 km^2 grid cells are neglected.

[27] The distribution of melt ponds on the Arctic ice is controlled by various factors such as surface temperature, cloud coverage, underlying ice type, as well as snow coverage. Melt pond development starts with the melting of snow. Meltwater of snow and ice is collecting in surface

depressions and other deformed structures. Compared to the much more irregular surface topography of multiyear ice, the plane and flat surfaces of first-year ice have the potential to host large and extended melt pond areas [*Fetterer and Untersteiner*, 1998; *Perovich et al.*, 2011b]. As melting develops, pond water drains through porous ice and cracks. *Yackel et al.* [2000] also describe the pond behavior and distribution on multiyear ice as smaller, deeper, and more numerous than on first-year ice.

[28] From the results displayed in Figure 2, it is apparent, that the spatial pattern of the melt pond distribution correlates with the atmospheric conditions: In 2007, a persistent dipole pressure anomaly with unusually high pressure over the Beaufort Sea and low pressure over central and western Siberia [*Stroeve et al.*, 2008] resulted in strong southerly winds from the Bering Strait across the North Pole, which transported warm air and warm water masses into the Arctic. Additionally, a high pressure system over the Beaufort and Chukchi Seas, formed in early June 2007 and persisted for 3 months, caused a predominant clear sky [*Stroeve et al.*, 2008], allowing more incoming shortwave radiation. The negative cloud cover anomaly in the Beaufort Sea region for June–August 2007 amounts up to −25% [*Schweiger et al.*, 2008]. Figure 2 displays an extensive melt during June to August exactly in this region. In 2011, a similar pressure field is observed, but it is not as strong and persistent as in 2007. The location of the high pressure center is shifted to the North of Greenland and the low pressure center is shifted to Alaska, so that winds blew east to west instead northward as in 2007 (NCEP Reanalysis data from http://www.esrl.noaa.gov/psd, accessed in November 2011). The distribution of melt ponds in Figure 2 (right) reflects this shift: A distinct formation of high melt pond fractions can be identified in the Beaufort Sea. The cloud cover anomalies in July 2011 as presented by J. Overland et al. (Temperature and clouds, 2011, available at http://www.arctic.noaa.gov/reportcard/temperature_clouds.html), display values of up to –20% and are located over the Beaufort Sea and the Central Arctic.

[29] On the other side, low clouds have also the capability to warm the surface and enhance surface melting. Therefore, the surface temperature would also be a suitable parameter for examining melt pond fractions. However, this relationship can not be investigated with optical remote sensing due to the presence of clouds, but would be worth to conduct further research on this.

[30] Our observations of a high fraction of melt ponds in an early stage of the melting cycle provide evidence for the hypothesis that the occurrence of negative cloud anomalies and thus increased input of solar radiation enhance the formation of melt ponds. In combination with a thinning Arctic sea ice coverage, containing an increasing fraction of first-year ice, the early appearance of melt ponds could have contributed to the extreme sea ice decline of the recent years.

5. Conclusions

[31] We have analyzed the temporal and spatial distribution of melt pond fraction in the Arctic for the years 2000–2011 derived from multispectral MODIS satellite data as described in *Rösel et al.* [2012]. The analysis of annual melt pond fractions shows a negative trend of −16.4% of the total melt pond area over the entire melt season, corresponding to the declining sea ice extent. In the years of extreme sea ice loss, 2007 and 2011, we observe a maximum in total melt pond area in mid-June to end June. From the temporal and spatial resolved trends (Figure 4d), an increase of relative melt pond fraction from 80° to 88°N in June and August is evident. This reflects a prolonged melt season and is accordant to the studies of *Markus et al.* [2009]. Additionally, the thermodynamic potential of the higher melt pond fraction may on its part in turn influence the length of the melt season.

[32] Our study provides strong evidence for the importance of early appearance of melt ponds. The melt pond data set introduced here is provided through the Integrated Climate Data Center (ICDC, http://icdc.zmaw.de/) and can be used to test and propose parameterizations for melt ponds in current sea ice models for a better representation of early summer sea ice melting and to observe the length of melt seasons.

[33] **Acknowledgments.** We thank the scientific editor and the two anonymous reviewers for their profound comments and suggestions. The work was funded by a scholarship of the International Max-Planck-Research-School for Maritime Affairs in Hamburg. Additional support was provided by the Cluster of Excellence CliSAP (EXC177), University of Hamburg, funded through the German Science Foundation (DFG).

References

Agarwal, S., W. Moon, and J. S. Wettlaufer (2011), Decadal to seasonal variability of Arctic sea ice albedo, *Geophys. Res. Lett.*, *38*, L20504, doi:10.1029/2011GL049109.

Birnbaum, G., W. Dierking, J. Hartmann, C. Lüpkes, A. Ehrlich, T. Garbrecht, and M. Sellmann (2009), The campaign MELTEX with research aircraft "Polar 5" in the Arctic in 2008, *Rep. Polar Mar. Res.*, *593*, 3–85.

Brandt, R. E., S. G. Warren, A. P. Worby, and T. C. Grenfell (2005), Surface albedo of the Antarctic sea ice zone, *J. Clim.*, *18*, 3606–3622.

Curry, J. A., J. L. Schramm, and E. E. Ebert (1995), Sea ice-albedo climate feedback mechanism, *J. Clim.*, *8*, 240–247.

Ehn, J. K., C. J. Mundy, D. G. Barber, H. Hop, A. Rossnagel, and J. Stewart (2011), Impact of horizontal spreading on light propagation in melt pond covered seasonal sea ice in the Canadian Arctic, *J. Geophys. Res.*, *116*, C00G02, doi:10.1029/2010JC006908.

Eicken, H., T. C. Grenfell, D. K. Perovich, J. A. Richter-Menge, and K. Frey (2004), Hydraulic controls of summer Arctic pack ice albedo, *J. Geophys. Res.*, *109*, C08007, doi:10.1029/2003JC001989.

Eisenman, I., and J. S. Wettlaufer (2009), Nonlinear threshold behavior during the loss of Arctic sea ice-albedo, *Proc. Natl. Acad. Sci. U. S. A.*, *106*, 28–32, doi:10.1073/pnas.0806887106.

Fetterer, F., and N. Untersteiner (1998), Observations of melt ponds on Arctic sea ice, *J. Geophys. Res.*, *103*, 24,821–24,835.

Fetterer, F., K. Knowles, W. Meier, and M. Savoie (2002), Sea Ice Index, http://nsidc.org/data/g02135.html, Natl. Snow and Ice Data, Boulder, Colo. [Updated 2009.]

Fetterer, F., S. Wilds, and J. Sloan (2008), Arctic Sea Ice Melt Pond Statistics and Maps, 1999, 2000, and 2001, http://nsidc.org/data/g02159.html, Natl. Snow and Ice Data, Boulder, Colo.

Flocco, D., D. L. Feltham, and A. K. Turner (2010), Incorporation of a physically based melt pond scheme into a sea ice component of a climate model, *J. Geophys. Res.*, *115*, C08012, doi:10.1029/2009JC005568.

Frey, K. E., D. K. Perovich, and B. Light (2011), The spatial distribution of solar radiation under a melting Arctic sea ice cover, *Geophys. Res. Lett.*, *38*, L22501, doi:10.1029/2011GL049421.

Grenfell, T., and G. Maykut (1977), The optical properties of ice and snow in the Arctic basin, *J. Glaciol.*, *18*, 445–463.

Grenfell, T. C., and D. K. Perovich (1984), Spectral albedos of sea ice and incident solar irradiance in the southern Beaufort Sea, *J. Geophys. Res.*, *89*, 3573–3580.

Holland, M. M., C. M. Bitz, and B. Tremblay (2006), Future abrupt reductions in the summer Arctic sea ice, *Geophys. Res. Lett.*, *33*, L23503, doi:10.1029/2006GL028024.

Howell, S. E., A. Tivy, T. Agnew, T. Markus, and C. Derksen (2010), Extreme low sea ice years in the Canadian Arctic Archipelago: 1998 versus 2007, *J. Geophys. Res.*, *115*, C10053, doi:10.1029/2010JC006155.

Itoh, M., J. Inoue, K. Shimada, S. Zimmermann, T. Kikuchi, J. Hutchings, F. McLaughlin, and E. Carmack (2011), Acceleration of sea-ice melting due to transmission of solar radiation through ponded ice area in the

Arctic ocean: Results of in situ observation from icebreakers in 2006 and 2007, *Ann. Glaciol.*, *52*(57), 249–260.

Kay, J. E., T. L'Ecuyer, A. Gettelmann, G. Stephens, and C. O'Dell (2008), The contribution of cloud and radiation anomalies to the 2007 Arctic sea ice extend minimum, *Geophys. Res. Lett.*, *35*, L08503, doi:10.1029/2008GL033451.

Kurtz, N. T., T. Markus, S. L. Farrell, D. L. Worthen, and L. N. Boisvert (2011), Observations of recent Arctic sea ice volume loss and its impact on ocean-atmosphere energy exchange and ice production, *J. Geophys. Res.*, *116*, C04015, doi:10.1029/2010JC006235.

Kwok, R., and N. Untersteiner (2011), The thinning of Arctic sea ice, *Phys. Today*, *41*, 36–41.

Levermann, A., et al. (2011), Potential climatic transitions with profound impact on Europe, *Clim. Change*, *110*, 845–878, doi:10.1007/s10584-011-0126-5.

Lindsay, R. W., J. Zhang, A. Schweiger, M. Steele, and H. Stern (2009), Arctic sea ice retreat in 2007 follows thinning trend, *J. Clim.*, *22*, 165–175, doi:10.1175/2008JCLI2521.1.

Lüthje, M., D. L. Feltham, P. D. Taylor, and M. G. Worster (2006), Modeling the summertime evolution of sea-ice melt postcalibration, *J. Geophys. Res.*, *111*, C02001, doi:10.1029/2004JC002818.

Markus, T., D. J. Cavalieri, M. A. Tschudi, and A. Ivanoff (2003), Comparison of aerial video and Landsat 7 data over ponded sea ice, *Remote Sens. Environ.*, *86*, 458–469.

Markus, T., J. C. Stroeve, and J. Miller (2009), Recent changes in Arctic sea ice melt onset, freezeup, and melt season length, *J. Geophys. Res.*, *114*, C12024, doi:10.1029/2009JC005436.

Maslanik, J., S. Drobot, C. Fowler, G. McPhee, W. Emery, and R. Barry (2007), On the Arctic climate paradox and the continuing role of atmospheric circulation in affecting sea ice conditions, *Geophys. Res. Lett.*, *34*, L03711, doi:10.1029/2006GL028269.

Maslanik, J., J. Stroeve, C. Fowler, and W. Emery (2011), Distribution and trends in Arctic sea ice age through spring 2011, *Geophys. Res. Lett.*, *38*, L13502, doi:10.1029/2011GL047735.

Nicolaus, M., S. Gerland, S. R. Hudson, S. Hanson, J. Haapala, and D. K. Perovich (2010), Seasonality of spectral albedo and transmittance as observed in the Arctic transpolar drift in 2007, *J. Geophys. Res.*, *115*, C11011, doi:10.1029/2009JC006074.

Notz, D. (2009), The future of ice sheets and sea ice: Between reversible retreat and unstoppable loss, *Proc. Natl. Acad. Sci. U. S. A.*, *106*, 20,590–20,595, doi:10.1073/pnas.0902356106.

Pederson, C. A., E. Roeckner, M. Lüthje, and J.-G. Winther (2009), A new sea ice albedo scheme including melt ponds for ECHAM5 general circulation model, *J. Geophys. Res.*, *114*, D08101, doi:10.1029/2008JD010440.

Perovich, D. K. (1996), The optical properties of sea ice, *Monogr. 96-1*, 25pp., Cold Reg. Res. and Eng. Lab., Hanover, N. H.

Perovich, D. K., and W. B. Tucker III (1997), Arctic sea-ice conditions and distribution of solar radiation during summer, *Ann. Glaciol.*, *25*, 445–450.

Perovich, D. K., W. B. Tucker III, and K. A. Ligett (2002a), Aerial observations of the evolution of ice surface conditions during summer, *J. Geophys. Res.*, *107*, (C10), 8048, doi:10.1029/2000JC000449.

Perovich, D. K., T. C. Grenfell, B. Light, and P. V. Hobbs (2002b), Seasonal evolution of the albedo of multiyear Arctic sea ice, *J. Geophys. Res.*, *107*, (C10), 8044, doi:10.1029/2000JC000438.

Perovich, D. K., B. Light, H. Eicken, K. F. Jones, K. Runciman, and S. V. Nghiem (2007), Increasing solar heating of the Arctic ocean and adjacent seas, 1979–2005: Attribution and role in the ice-albedo feedback, *Geophys. Res. Lett.*, *34*, L19505, doi:10.1029/2007GL031480.

Perovich, D. K., J. A. Richter-Menge, K. F. Jones, and L. Bonnie (2008), Sunlight, water, and ice: Extreme Arctic sea ice melt during the summer of 2007, *Geophys. Res. Lett.*, *35*, L11501, doi:10.1029/2008GL034007.

Perovich, D. K., T. C. Grenfell, B. Light, B. C. Elder, J. Harbeck, C. Polashenski, W. B. Tucker III, and C. Stelmach (2009), Transpolar observations of the morphological properties of Arctic sea ice-albedo, *J. Geophys. Res.*, *114*, C00A04, doi:10.1029/2008JC004892.

Perovich, D. K., J. A. Richter-Menge, K. F. Jones, B. Light, B. C. Elder, C. Polashenski, D. Laroche, T. Markus, and R. Lindsay (2011a), Arctic sea-ice melt in 2008 and the role of solar heating, *Ann. Glaciol.*, *52*(57), 355–359.

Perovich, D. K., K. F. Jones, B. Light, H. Eicken, T. Markus, J. Stroeve, and R. Lindsay (2011b), Solar partitioning in a changing Arctic sea-ice cover, *Ann. Glaciol.*, *52*(57), 192–196.

Rösel, A., and L. Kaleschke (2011), Comparison of different retrieval techniques for melt ponds on Arctic sea ice from Landsat and MODIS satellite data, *Ann. Glaciol.*, *52*(57), 185–191.

Rösel, A., L. Kaleschke, and G. Birnbaum (2012), Melt ponds on Arctic sea ice determined from MODIS satellite data using an artificial neuronal network, *Cryosphere*, *6*, 1–19, doi:10.5194/tc-6-1-2012.

Sankelo, P., J. Haapala, I. Heiler, and R. Eero (2010), Melt pond formation and temporal evolution at the station Tara during summer 2007, *Polar Res.*, *29*, 311–321, doi:10.1111/j.1751-8369.2010.00161.x.

Schweiger, A. J., J. Zhang, R. W. Lindsay, and M. Steele (2008), Did unusually sunny skies help drive the record sea ice minimum of 2007?, *Geophys. Res. Lett.*, *35*, L10503, doi:10.1029/2008GL033463.

Scott, F., and D. L. Feltham (2010), A model of the three-dimensional evolution of Arctic melt ponds on first-year and multiyear sea ice, *J. Geophys. Res.*, *115*, C12064, doi:10.1029/2010JC006156.

Serreze, M. C. (2011), Rethinking the sea-ice tipping point, *Nature*, *471*, 47–48, doi:10.1038/471047a.

Serreze, M. C., and R. G. Barry (2011), Processes and impacts of Arctic amplification: A research synthetis, *Global Planet. Change*, *77*, 85–96, doi:10.1016/j.gloplacha.2011.03.004.

Serreze, M. C., A. P. Barrett, and J. J. Cassano (2011), Circulation and surface controls on the lower tropospheric air temperature field of the Arctic, *J. Geophys. Res.*, *116*, D07104, doi:10.1029/2010JD015127.

Skyllingstad, E. D., C. A. Paulson, and D. K. Perovich (2009), Simulation of melt pond evolution on level ice, *J. Geophys. Res.*, *114*, C12019, doi:10.1029/2009JC005363.

Stroeve, J., M. Serreze, S. Drobot, S. Gearheard, M. Holland, J. Maslanik, W. Meier, and T. Scambos (2008), Arctic sea ice extent plummets in 2007, *Eos Trans. AGU*, *89*(2), 13, doi:10.1029/2008EO020001.

Tschudi, M. A., J. A. Maslanik, and D. K. Perovich (2008), Derivation of melt pond coverage on arctic sea ice using MODIS observation, *Remote Sens. Environ.*, *112*, 2605–2614.

Walsh, J. E., W. E. Chapman, and D. H. Portis (2009), Arctic cloud fraction and radiative fluxes in atmospheric reanalysis, *J. Clim.*, *22*, 2316–2334, doi:10.1175/2008JCLI2213.1.

Warren, S. G. (1982), Optical properties of snow, *Rew. Geophys.*, *20*, 67–89.

Yackel, J. J., D. G. Barber, and J. M. Hanesiak (2000), Melt ponds on sea ice in the Canadian Archipelago: 1. Variability in morphological and radiative properties, *J. Geophys. Res.*, *105*(C9), 22,049–22,060, doi:10.1029/2000JC900076.